

## Late Quaternary sedimentation in the Ulleung Interplain Gap, East Sea (Korea)

S.H. Lee<sup>a,\*</sup>, J.J. Bahk<sup>b</sup>, S.K. Chough<sup>a</sup>, G.G. Back<sup>c</sup>, H.S. Yoo<sup>b</sup>

<sup>a</sup>*School of Earth and Environmental Sciences, Seoul National University, Seoul 151-742, South Korea*

<sup>b</sup>*Marine Geoenvironment and Resources Research Division, Korea Ocean Research and Development Institute, Ansan P.O. Box 29, Seoul 425-600, South Korea*

<sup>c</sup>*National Oceanographic Research Institute, Incheon 400-037, South Korea*

Received 4 March 2003; received in revised form 9 February 2004; accepted 5 March 2004

### Abstract

The Ulleung Interplain Gap (UIG) is a deep (2300–2700 m) passage which has served as a conduit for deep-water circulation between the Ulleung and Japan basins. A detailed analysis of Chirp (2–7 kHz) subbottom profiles (ca. 6270 line-km) and nine sediment cores (8.6–11.4 m long) together with age data of tephra layers and four AMS <sup>14</sup>C from the UIG and the adjacent areas reveals complex sedimentation caused by an interaction between bottom currents and mass flows during the last- and post-glacial periods. From high-resolution subbottom data, rock basement, slide/slump/rock-fall deposits, mass-flow chutes/channels, mass-flow deposits, bottom-current deposits, and a large-scale bottom-current channel system are recognized. Core sediments consist of various deposits of turbidites, muddy contourites, manganiferous contourites, and pelagic/hemipelagic sediments. Based on vertical distribution of sedimentary facies together with a chronostratigraphic framework, core sediments can be divided into Units I (< ~ 15 ka) and II (> ~ 15 ka).

The extensive mass-flow deposits with slope failures on the entire slopes of topographic highs around the UIG and the dominant turbidites in Unit II (> ~ 15 ka) suggest that a relatively large amount of sediment was delivered into the UIG by frequent mass flows (recurrence intervals of ca. 250–500 years in the upper Unit II) during the last-glacial period. Erosion or hampered sedimentation by bottom currents is indicated by the truncated reflectors of channel walls and muddy/manganiferous contourites in the Ulleung Interplain Channel (UIC) along the UIG. Interbedded turbidites in the UIC floor reflect that some large-scale mass flows intermittently entered into the UIC.

The UIC has an asymmetric channel-flank geometry. The southeastern flank shows a gentle, wide mound morphology of mass-flow deposits derived from large-scale slope failures on the slopes of the Oki Bank, reflecting a dominance of downslope gravitational processes over alongslope bottom currents. In contrast, the northwestern flank is characterized by a narrow, steep geometry of mass-flow deposits, where a relatively small amount of sediment derived from the slopes of the South Korea Plateau could not overcome bottom-current activity.

The dominant muddy and manganiferous contourites with rare turbidites in Unit I (< ~ 15 ka) reflect intensified bottom currents and infrequent slope failures (recurrence intervals of ca. 1700–5000 years) during the post-glacial period. These

\* Corresponding author. Present address: Challenger Division, Southampton Oceanography Centre, Southampton SO14 3ZH, UK.  
E-mail addresses: shlee@soc.soton.ac.uk, sanglee@kordi.re.kr (S.H. Lee).

conditions facilitated the formation of a thin, elongate mound of bottom-current drifts overlying mass-flow deposits on the southeastern UIC flank, and sustained erosion or hampered sedimentation in the UIC.

© 2004 Elsevier B.V. All rights reserved.

*Keywords:* deep passage; bottom current; turbidity current; debris flow; Ulleung Interplain Gap; East Sea (Sea of Japan)

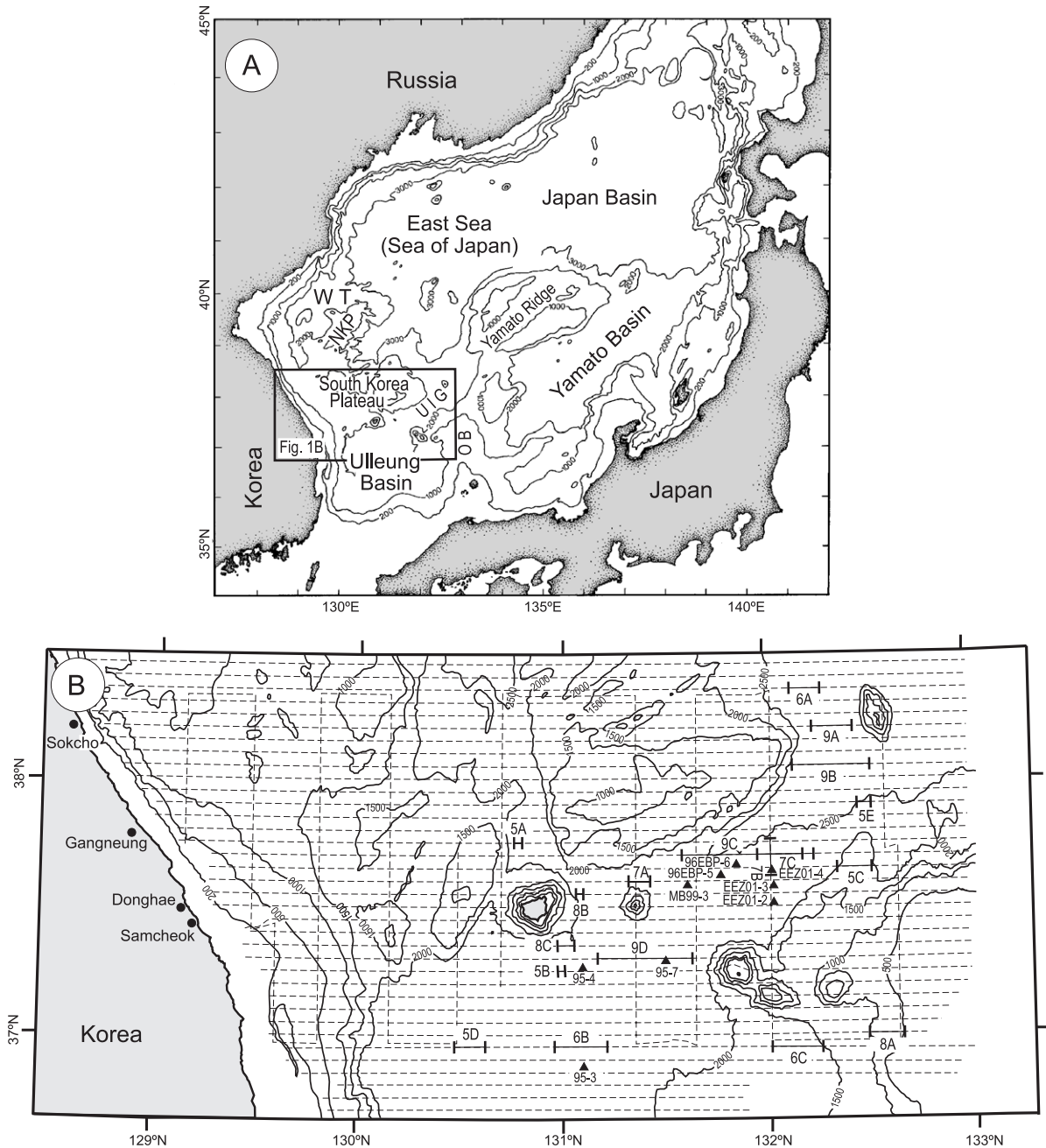
## 1. Introduction

Deep passages, constricted by topographic highs, usually serve as conduits for deep-water circulation between ocean basins, e.g., Vema Channel and São Paulo Abyssal Gap (Johnson, 1984; Mézerais et al., 1993; Faugères et al., 1998), Kane Gap (Meinert, 1986), Samoan Passage (Hollister et al., 1974), Amirante Passage (Johnson and Damuth, 1979; Johnson et al., 1983), Shag Rocks Passage (Howe et al., 1997; Howe and Pudsey, 1999), and Valerie Passage (McCave and Carter, 1997). Bottom-water circulation is constrained through deep passages so that flow velocities are markedly increased. In deep passages, a weak supply of sediment from neighbouring topographic highs results in the dominant influence of bottom currents on the deposits (Hollister et al., 1974; Johnson, 1984; Mézerais et al., 1993; McCave and Carter, 1997; Faugères et al., 1999). The passage floor is characterized by significant erosion or non-deposition, forming an axial channel or moat system (Johnson and Damuth, 1979; Johnson et al., 1983; Faugères et al., 1993). In addition, irregular patches of lateral or channel-related drifts form on the floor and flanks of the channel system (Johnson and Damuth, 1979; Johnson, 1984; Faugères et al., 1999). Further down-current, contourite fans often accumulate at the exit of channel system (Mézerais et al., 1993; Faugères et al., 1998).

Where a large amount of sediment is delivered into a deep passage from adjacent topographic highs by downslope gravitational processes, depositional character may be very complex. The interaction of bottom currents and mass flows is common along deep-water continental margins (Faugères et al., 1999). The interaction has been well documented on the western margins of the Atlantic Ocean (Tucholke and Mountain, 1986; McMaster et al., 1989; Locker and Laine, 1992; Massé et al., 1998), the eastern New Zealand margin (Carter and McCave, 1997; McCave and

Carter, 1997; Carter, 2001), the Rockall continental margin off NW Britain (Howe, 1996; Armishaw et al., 1998; Stoker, 1998) and the continental rise of the Antarctic Peninsula (Rebesco et al., 1996; Nitsche et al., 2000). The distinction between bottom-current and mass-flow deposits is, however, difficult as the interaction of the two sedimentary processes generally forms complicated patterns of sedimentary features in both time and space. In order to discriminate between bottom-current and mass-flow deposits, detailed description of sedimentary features from all available data is necessary (e.g., Howe, 1996; McCave and Carter, 1997; Armishaw et al., 1998; Massé et al., 1998).

The Ulleung Interplain Gap (UIG) is a deep (ca. 2500 m deep and 75 km wide) passage between the Japan and Ulleung basins (Chough et al., 2000; Figs. 1A and 2). It has served as a conduit for deep-water circulation from the Japan to Ulleung basins. The deep water has originated from winter cooling of surface waters in the northern part of the East Sea (Sea of Japan) off Vladivostok (Gamo et al., 1986; Kim et al., 1991, 2002; Kawamura and Wu, 1998; Chang et al., 2002; Senjyu et al., 2002). Influence of bottom currents in the UIG was postulated by the presence of an erosional channel system (Ulleung Interplain Channel, UIC) (Chough et al., 1985, 2000). The UIC is up to 13.5 km wide and 15–85 m deep, and cuts into the underlying stratified sequences. In addition to bottom currents, large areas of slope-failure morphology on the neighbouring topographic highs highlight the influence of mass flows (Lee, 2001). Recent acquisition of large amounts (ca. 6270 km) of dense- and regular-spaced (ca. 5.5 km intervals), high-resolution (2–7 kHz) subbottom profiles and nine (8.6–11.4 m long) piston cores in the UIG and the adjacent areas (Fig. 1B) provides an unprecedented database for revealing the complex sedimentation caused by interaction between bottom currents and mass flows in the deep passage. This



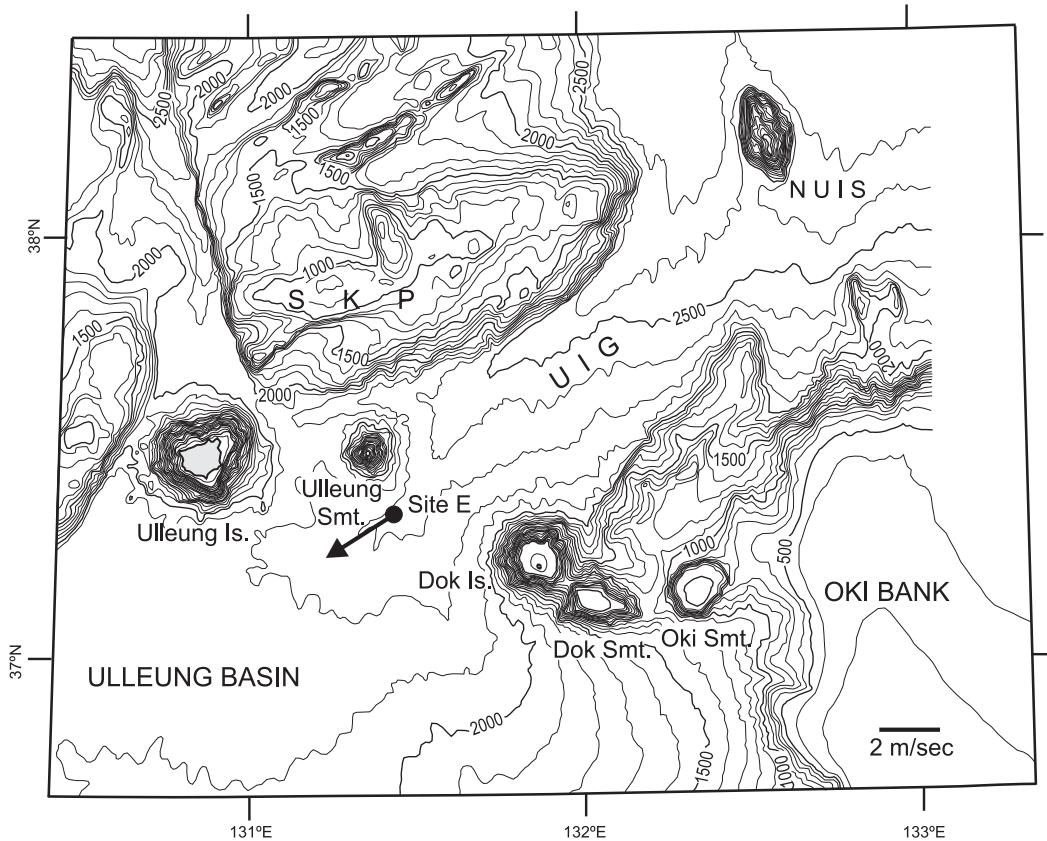


Fig. 2. Detailed bathymetric and physiographic features of the Ulleung Interplain Gap and the adjacent areas. Note a southwestward mean current vector of deep water (1920–2360 m water depth) at the southern exit (Site E) of the UIG during November 1996–October 1997 and November 1999–May 2000 (Chang et al., 2002). Bathymetry in metres. NUIS=North Ulleung Interplain Seamount; SKP=South Korea Plateau; Smt. = Seamount; UIG=Ulleung Interplain Gap.

paper details sedimentary character and geometry of sediment bodies in the UIG and the adjacent topographic highs, and proposes a depositional model for deep passages where bottom currents have interacted with mass flows.

## 2. Geological and oceanographic setting

The East Sea (Sea of Japan) is a semi-enclosed back-arc basin surrounded by the east Asian continent and the Japanese Islands (Fig. 1A). It was formed by an extension of continental crust accompanied with a progressive drift of the Japanese Arc during the late Oligocene to early Miocene (Jolivet et al., 1995; Yoon and Chough, 1995). The East Sea consists of three

deep basins (Ulleung, Japan and Yamato basins) separated by the Korea Plateau, Oki Bank and Yamato Ridge (Fig. 1A). The Ulleung Basin gradually deepens northeastward from 2000 to 2300 m and is connected to the deep Japan Basin through the Ulleung Interplain Gap (UIG) (Figs. 1A and 2). The UIG is bounded in the southeast by the slopes of the Oki Bank and Dok Island, and in the northwest by an ENE–WSW-trending escarpment of the South Korea Plateau (Fig. 2). In the UIG, a deep-sea channel system (Ulleung Interplain Channel, UIC) occurs along the base-of-slope of the South Korea Plateau (Chough et al., 1985, 2000). The UIG is punctuated by the Ulleung Seamount and North Ulleung Interplain Seamount in the southwestern and northeastern parts, respectively (Fig. 2).

The East Sea is connected to the North Pacific and adjacent seas through four shallow and narrow straits (water depths of 12–140 m). Because of the shallow depths of the straits, water exchanges with adjacent seas are limited to the upper 200 m depth, where the Tsushima Current, a branch of the warm saline Kuroshio Current, enters the East Sea through the Korea Strait and flows out through the Tsugaru and Soya straits (Moriyasu, 1972). Below the surface layer is present a quite homogeneous water mass which has a nearly constant low temperature of 0–1 °C. The water mass, named the East Sea (Japan Sea) Proper Water (ESPW) after Uda (1934), is known to be rich in dissolved oxygen (5–7 ml/l), and has renewed quickly within a few hundred years by a wintertime sinking of cold, oxygen-rich surface seawater in the northern part of the East Sea off Vladivostok (Gamo and Horibe, 1983; Gamo et al., 1986; Watanabe et al., 1991; Seung and Yoon, 1995; Kawamura and Wu, 1998). Although details of the deep-water circulation pattern and current strength are poorly known due to the scarcity of direct current measurements, it is certain that the ESPW of the Ulleung Basin has been brought into the basin from the north (i.e., Japan Basin) because the sea surface temperature does not fall below 8 °C in the Ulleung Basin (Kim et al., 1991). The UIG has been proposed as the main conduit of the deep water entering the Ulleung Basin (Kim et al., 1991). Recently achieved mooring data from the southern exit of the UIG for 19 months display that currents at 1920–2360 m water depth dominantly flow southwestward with speeds of 0.08–14.31 cm/s (average speeds: ca. 2.4 cm/s) (Chang et al., 2002; Fig. 2, Site E).

The deep-water circulation in the East Sea has experienced significant fluctuations. For example, the bottom-water formation in the East Sea has become less active for the last 40 years, which is supported by a significant decrease in oxygen concentrations in deep waters accompanied with deepening of the oxygen minimum depth by more than 1000 m (Gamo et al., 1986; Kim and Kim, 1996; Kim et al., 1999; Gamo, 1999). Recent observations, however, report a sudden initiation of bottom-water formation in the northwestern part of the sea after a severely cold winter in 2000–2001 (Kim et al., 2002; Senjyu et al., 2002). The new bottom-water formation contributes the acceleration of deep thermohaline circulation in the East Sea (Senjyu et al., 2002). During the last deglaciation, the East Sea has undergone a drastic change in bottom-water oxygen concentration. Geochemical and paleontological evidences from sediment cores indicate that an anoxic bottom-water condition prevailed during the Last Glacial Maximum when sea level was lowered by as much as 120 m (Oba et al., 1991; Crusius et al., 1999). Based on oxygen isotope data, the anoxia were attributed to a decrease in surface-water salinity by freshwater input and consequently intensified water-column stratification in the nearly isolated East Sea (Oba et al., 1991; Keigwin and Gorbarenko, 1992; Gorbarenko and Southon, 2000).

### 3. Data and methods

The National Oceanographic Research Institute (NORI) of Korea conducted a reconnaissance survey from 1996 to 1997 for regional seafloor mapping of

Table 1  
Location, water depth and length of sediment cores

Core number	Water depth (m)	Location		Physiography	Core length (cm)	Reference
		Latitude	Longitude			
95-3	2151	36°52.5N	131°04.7E	Basin plain of the UB	1088	Bahk et al. (2000)
95-4	2197	37°15.2N	131°06.3E	Basin plain of the UB	985	Bahk et al. (2000)
95-7	2295	37°16.8N	131°29.4E	UIC floor	856	Bahk et al. (2001)
96EBP-5	2370	37°37.7N	131°46.5E	UIC wall	1060	Bahk et al. (2001)
96EBP-6	2462	37°39.1N	131°51.2E	Lower slope of the OB	1140	Bahk et al. (2001)
MB99-3	2435	37°35.7N	131°37.8E	UIC floor	910	This study
EEZ01-2	2210	37°30.5N	132°03.0E	Lower slope of the OB	1032	This study
EEZ01-3	2288	37°35.7N	132°03.2E	Lower slope of the OB	948	This study
EEZ01-4	2344	37°39.4N	132°02.9E	Lower slope of the OB	997	This study

OB = Oki Bank; UB = Ulleung Basin; UIC = Ulleung Interplain Channel.

Table 2  
AMS  $^{14}\text{C}$  dates of planktonic foraminifera

Core number	Depth (cm)	Laboratory	Lab number	$^{14}\text{C}$ age <sup>a</sup> (years BP)	Reference
95-4	310	Center for AMS, Lawrence Livermore National Laboratory	28884	15,090 ± 200	Bahk et al. (2000)
96EBP-6	374	AMS Lab of Seoul National University	SNU99-071	14,480 ± 170	Bahk et al. (2001)
96EBP-6	445	AMS Lab of Seoul National University	SNU99-067	17,320 ± 560	Bahk et al. (2001)
MB99-3	252	Leibniz Laboratory, University of Kiel	KIA11591	15,470 ± 80	This study

<sup>a</sup> No reservoir corrections have been applied.

the East Sea. During the 1997 cruise, 12739 km of high-resolution subbottom profiles were collected in the area of 36°48'N–38°27'N and 128°30'E–133°00'E using a Chirp sonar system (Fig. 1B). Bathymetric data were concurrently acquired using a multi-beam echo sounder system (SeaBeam 2100). In this study, we use about 6270 km of Chirp subbottom profiles in the Ulleung Interplain Gap, Oki Bank and Ulleung

Basin. The survey lines were mostly aligned in an E–W direction with a space of approximately 5.5 km intervals. The Chirp sonar system (Datasonics CAP-6000W) is a tuned-frequency profiler that emits a computer-generated FM swept pulse with a frequency band of 2–7 kHz as a source signal. Returning signals were processed using a matched-filter correlation technique in order to collect a frequency band of 2–

Table 3  
Description and interpretation of sedimentary facies in core sediments

Facies	Description	Interpretation
Massive gravelly sand (MGS)	Usually medium- to thick-bedded; generally include abundant pumice lapilli with a few mud balls; massive to stratified; either ungraded or graded; sharp, often deformed lower boundary; either sharp or gradational upper boundary	Coarse-grained, volcanoclastic turbidites (Stow et al., 1996)
Laminated sand and silt (LS)	Generally thin-bedded; horizontally or cross-laminated; overall normal grading; horizontal or inclined sharp lower boundary; sharp or gradational upper boundary	Fine-grained turbidites: Bouma's (1962) T <sub>c</sub> or T <sub>d</sub> divisions
Laminated silty mud (LM)	Thin-bedded; laminated with silt–clay couplets; normally graded; sharp lower boundary; gradational upper boundary	Fine-grained turbidites: Piper's (1978) E <sub>1</sub> division
Crudely laminated mud (CLM)	Thin-bedded; randomly scattered foraminifera; crude laminae characterized by strings of silt and diatom aggregates; sharp upper and lower boundaries	Pelagic/hemipelagic sediments formed under poorly oxygenated bottom-water condition (Bahk et al., 2000)
Homogeneous mud (HM)	Thin- to medium-bedded; lack of visible primary structures; gradational lower boundaries with facies LM or LS	Fine-grained turbidites: Piper's (1978) E <sub>2</sub> division
Indistinctly layered mud (ILM)	Medium- to thick-bedded; an alternation of greenish gray mud and olive to light gray mud with indistinct irregular boundaries; no systematic vertical variations in layer thickness and frequency	Manganiferous contourites; metal enrichments associated with hampered sedimentation by bottom currents (Stow et al., 1998)
Bioturbated mud (BM)	Variable in thickness; characterized by burrows and pyrite filaments; often associated with facies ILM	Pelagic/hemipelagic sediments formed under well-oxygenated bottom-water condition (Bahk et al., 2000); muddy contourites (Stow et al., 1998)
Bioturbated sandy or silty mud (BSM)	Thin-bedded; bioturbated; diffuse upper and lower boundaries	Bioturbation of fine-grained turbidites after deposition
Laminated Mn-carbonate mud (CaM)	Thin-bedded; composed mostly of Mn-carbonate crystallites; underlain by facies CLM and overlain by facies ILM	Chemogenic sediments formed under changing bottom-water conditions from anoxic to oxic (Bahk et al., 2001)

Summarized from Bahk et al. (2000, 2001).

7 kHz, which provides higher resolution images than those of the 3.5-kHz system (Schock et al., 1989; LeBlanc et al., 1992). Navigation was controlled using a Differential Global Positioning System (Trimble 4000RS/DS) whose accuracy of position is within 10 m.

In order to provide ground truth for high-resolution echo characters and age data, we use nine (8.6–11.4 m long) piston cores acquired by the Korea Ocean Research and Development Institute during 1995–2001 cruises (Table 1 and Fig. 1B). X-radiographs of 1-cm-thick slabs were taken on the halves of lengthwise-cut split cores to observe macroscopic sedimentary structures. Grain-size analysis was conducted using standard sieves and a Micrometrics Sedigraph 5100 for sand and mud fractions, respectively. Four AMS  $^{14}\text{C}$  dates of planktonic foraminifera from the selected cores were obtained (Table 2). Analytical methods of grain size, sedimentary structures, compositions and AMS  $^{14}\text{C}$  dating were detailed in Bahk et al. (2000, 2001).

#### 4. Sedimentary facies and stratigraphy of core sediments

On the basis of sedimentary structures, grain size, and composition, core sediments are classified into nine sedimentary facies (Table 3). Sedimentary features and interpretation of each facies are detailed in Table 3 and Fig. 3.

The correlation among the cores is made mainly based on lithologic changes and tephra layers of age-known eruptions with four AMS  $^{14}\text{C}$  dates (Table 2 and Fig. 4). The distribution of sedimentary facies shows that in most cores, except core MB99-3 where massive gravelly sand (facies MGS) predominates, the upper part is dominated by bioturbated mud (facies BM) which represents post-glacial (< ~ 15 ka) pelagic/hemipelagic sedimentation under well-oxygenated bottom-water conditions (Fig. 4). Thickness of the bioturbated mud (facies BM)-dominated upper interval (Unit I, hereafter) is variable from 1.3 to 4.2 m with maximum in core EEZ01-4. The

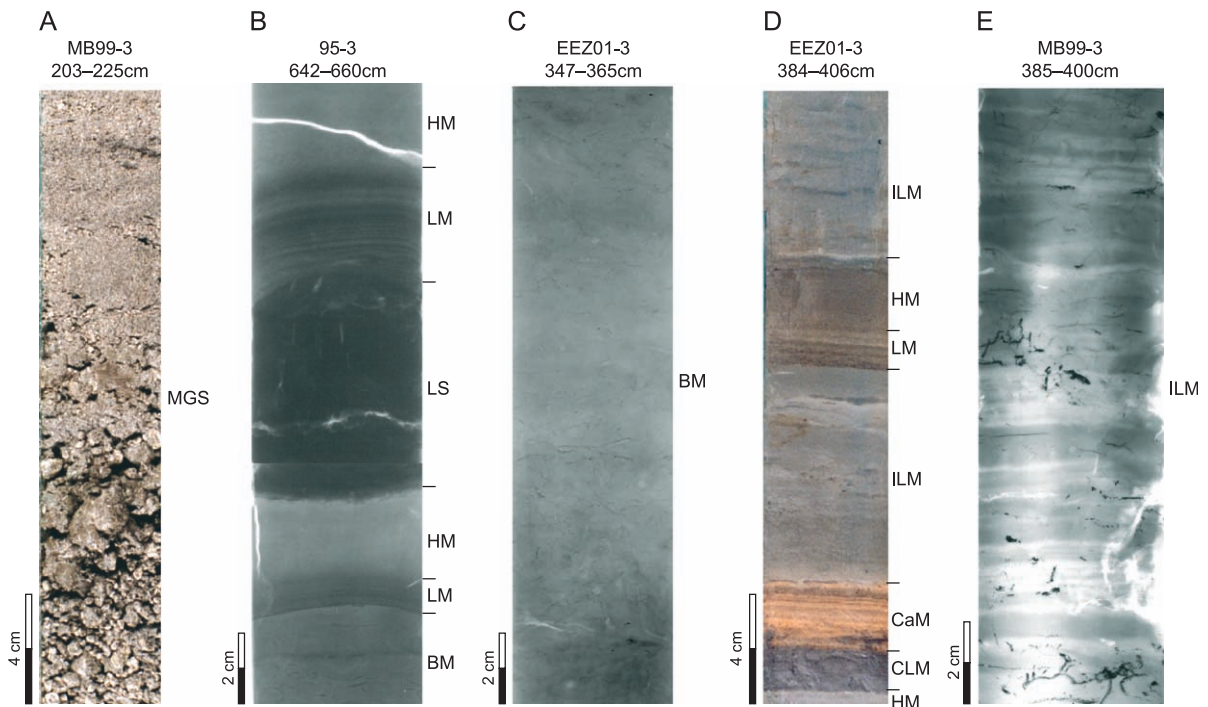
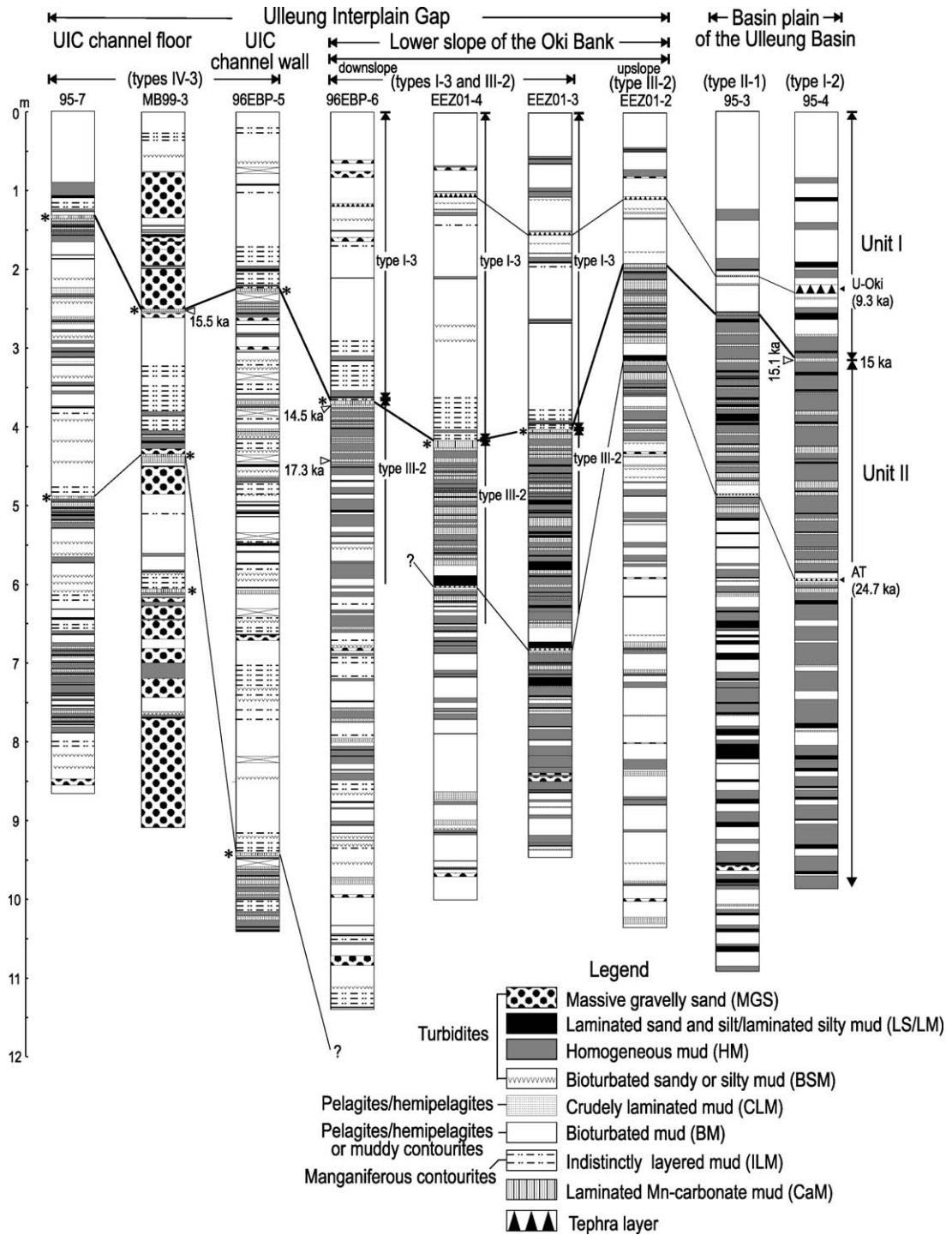


Fig. 3. X-radiographs (B, C and E) and photographs (A and D) of selected core sections. For symbols on the right side, see Table 3. Core locations are shown in Fig. 1B.





intervals below Unit I (Unit II, hereafter) generally consist of alternating fine-grained turbidites (facies LS, LM and HM) and pelagic/hemipelagic sediments (facies BM and CLM), and show considerable lithologic variations among the cores (Fig. 4). In most cores, the upper part of Unit II is characterized by repetitive sequences of fine-grained turbidites (facies LS, LM, and HM) and non-bioturbated pelagic/hemipelagic sediments (facies CLM) which represent anoxic bottom-water and unstable slope conditions during the Last Glacial Maximum (Lee et al., 1996; Bahk et al., 2000). In cores from the UIG, a laminated Mn-carbonate mud (facies CaM) layer occurs at the boundary between Units I and II (Fig. 4), indicating an abrupt oxygenation of bottom water during the last deglaciation (Bahk et al., 2001). The proportions of turbidite beds in Unit II are greatest in the basin plain and the lower slope of the Oki Bank, and significantly decrease in the floor and walls of the UIC (Fig. 4). It is also notable that in cores from the UIC, laminated Mn-carbonate mud (CaM) layers occur once or twice below the anoxic intervals of the last glacial maximum period (Fig. 4). The CaM layers most likely represent anoxic to oxic change in bottom water before the last glacial maximum which were not recorded in cores from the basin plain and slope of the Oki Bank, and imply significant overall reduction of sedimentation rates in the UIC region. The lowered sedimentation rates in the UIC are also supported by frequent occurrence of the ‘manganiferous contourite’ (facies ILM) which indicates hampered sedimentation by bottom currents (Fig. 4).

## 5. Echo types

Ten echo types are identified on the basis of clarity, continuity and geometry of bottom and subbottom echoes, as well as seafloor morphology (Table 4). These types are classified into four major classes: (1) distinct echoes (types I-1, I-2, and I-3), (2) indistinct echoes (types II-1 and II-2), (3) hyperbolic or wavy

echoes (types III-1 and III-2), and (4) combined echoes (types IV-1, IV-2, and IV-3). Acoustic features and interpretation of each type are detailed in Table 4 and Figs. 5–9.

## 6. Distribution of echo and lithologic characters

### 6.1. Ulleung Island and Seamount, and North Ulleung Interplain Seamount (NUIS)


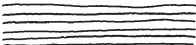





Both the Ulleung Island and Seamount and the NUIS are dominated by type III-1 (basement highs or outcrops) (Fig. 10). Here, the topographic depressions (small-scale gullies) between the hyperbolae are partly covered by small-scale, thin masses of type IV-1 (slides, slumps and rock falls). The lower to middle slopes dominantly comprise slides, slumps and rock falls (type IV-1) (Fig. 10). These mass-movement deposits are transitional downslope to types II-2 (debrites), I-1 (debrites/turbidites), and I-2 (turbidites) (Fig. 10). In the lower slopes of the Ulleung Island and Seamount, type IV-2 (mass-flow chutes/channels) occurs (Fig. 10). These chutes and channels are 2–6.8 km wide and < 15 m deep, and decrease downslope in relief.

### 6.2. Escarpment of the South Korea Plateau

The escarpment of the South Korea Plateau is dominated by types III-1 (basement highs or outcrops) and IV-1 (slides, slumps and rock falls) (Fig. 10). Type III-1 with partial cover of small-scale, thin masses of type IV-1 occurs in the steeper slope areas, whereas type IV-1 is present on the gentler slopes connected to the intervening troughs in the South Korea Plateau (Lee et al., 2002). Slide and slump deposits (type IV-1) change downslope to mass-flow deposits (type I-1), turbidites (types I-2 and II-1) and mass-flow chutes/channels (type IV-2) (Fig. 10). Type II-1 (turbidites) in the northeastern lower slope of the plateau is truncated by type IV-3 (large-scale bottom-current channel system) (Fig. 9A).

Fig. 4. Summary of sedimentary logs and correlation of cores. For location of cores, see Figs. 1B, 7B, 9D and 10. Solid triangles indicate tephra layers of known eruption ages (Machida, 1999; Gorbarenko and Southon, 2000). U-Oki = Ulleung-Oki tephra (9.3 ka); AT = Aira-Tn tephra (24.7 ka). Open triangles represent AMS  $^{14}\text{C}$  dates. Asterisks in cores from the Ulleung Interplain Gap denote the layers of ‘laminated Mn-carbonate mud’ (facies CaM). For detailed acoustic characters of echo types (types I-2, I-3, II-1, III-2 and IV-3), see Table 4.

Table 4  
Description and interpretation of echo types

Class	Type	Line drawing	Description	Occurrence	Interpretation
I	I-1		Very sharp bottom echoes with nearly flat to slightly irregular topography; strongly reflective, prolonged subbottom echoes with locally intermittent, discontinuous internal reflectors; shallow (<15 m) penetration depth	Lower slopes of the Ulleung Seamount and Island and the escarpment of the South Korea Plateau	Coarse-grained, volcanoclastic mass-flow deposits (Chough et al., 1985)
	I-2		Distinct bottom echoes and several discrete, continuous, parallel internal reflectors; 15–80 m in penetration depth; nearly flat surface topography; a filling geometry in the topographic depressions; a few small-scale (0.7–1 km wide, <10 m deep), intermittent channel-levee systems; a N–S or NNW–SSE orientation of channel-levee systems; northward decrease in channel relief; continuous aggrading reflectors in the levees; in the topographic highs (upper slope and ridge summits in the Oki Bank), slightly to steeply inclined surface topography	Basin plain of the Ulleung Basin; distal lower slopes of the volcanic islands and seamounts and the northern Oki Bank; upper slope and ridge summits in the Oki Bank	Turbidites with a few depositional channel-levee systems (Damuth, 1980; Flood and Damuth, 1987); pelagic/hemipelagic sediments (Yoon et al., 1996; Lee et al., 2002)
					
I-3		An uppermost transparent layer which is discordant to internal reflectors of the underlying sedimentary sequences; locally, vague or indistinct, discontinuous internal reflectors in the transparent layer; 3–6 m in thickness; lateral decrease in thickness, forming a mound shape in cross section; a NE–SW-trending elongate distribution along the Ulleung Interplain Channel	Southeastern flank of the Ulleung Interplain Channel	Bottom-current deposits (Howe, 1996; Faugères et al., 1999)	
II	II-1		Indistinct to prolonged bottom echoes with either no or a few sub-parallel, intermittent internal reflectors; nearly flat surface topography; a filling geometry in the topographic depressions; 20–40 m in penetration depth; a few small-scale (0.3–1 km wide, less than 5 m deep), intermittent channel-levee systems showing lobate geometry in cross section; a N–S or NNW–SSE orientation of channel-levee systems; northward reduction in channel relief; continuous aggrading reflectors in the levees	Basin plain of the Ulleung Basin; distal lower slopes of the northeastern South Korea Plateau and the northern Oki Bank	Turbidites with a few depositional channel-levee systems (Clark and Pickering, 1996; Chough et al., 1997)
					
	II-2		Laterally wedged, acoustically transparent masses; various bottom echoes ranging from weak through very prolonged to small-scale hummocky echoes; either convex-up or nearly flat upper surfaces with concave-up bases; 3–25 m in thickness; downslope decrease in thickness	Lower slopes of the Oki Bank and the volcanic islands and seamounts	Debris-flow deposits (Embley, 1976; Lee et al., 1999)

III	III-1		Large single or irregular overlapping hyperbolae with widely varying vertex elevation (up to 200–300 m) above the seafloor; highly variable dimensions of the hyperbolae; very strong surface echoes and prolonged subbottom echoes of the hyperbolae; locally covered by small-scale, thin blocky or hyperbolic masses (type IV-1)	Volcanic islands and seamounts, and the escarpment of the South Korea Plateau	Basement highs or outcrops (Damuth, 1980; Laine et al., 1986)
	III-2		Regular to slightly irregular wavy bottom echoes with upslope migrating subbottom reflectors in downslope-parallel section; in contour-parallel section, irregular and less wavy forms; parallel orientation of the wave crests to the regional slope; asymmetric wave geometry with steeper, thicker upslope and gentler, thinner downslope flanks; waves: 0.3–2 km in wavelength, less than 15 m in height; gradual downslope reduction in wave height, changing to nearly flat surface topography; progressive downslope decrease in thickness and wave asymmetry; mostly overlain by type I-3	Lower slopes of the Oki Bank and Dok Island	Fine-grained turbidity-current sediment waves (Normark et al., 1980; Wynn et al., 2000a; Wynn and Stow, 2002)
IV	IV-1		Irregular blocky, lumpy or hyperbolic masses bounded upslope by scarps or scars; a few metres to 90 m in scarp relief; highly variable degree of internal deformation in the displaced masses; scars marked by either a sharp glide plane or irregular drape of thin acoustically transparent or hyperbolic masses; several scarps below the headwall scarp; step-like geometry of failed masses; locally, strongly reflective, slightly irregular to regular overlapping hyperbolae (0.3–1.2 km wide) with slightly varying vertex elevation (<10 m) above the seafloor	Upper to lower slopes of volcanic islands and seamounts, the Oki Bank, and the escarpment of the South Korea Plateau	Slide, slump and rock-fall deposits with slope-failure scars (Embley and Jacobi, 1977; Nardin et al., 1979; Chough et al., 1985)
	IV-2		Various echo characters on the channelized geometry; channel floors: nearly flat to convex-up, sharp, prolonged or small-scale hummocky bottom echoes with either transparent or rare intermittent, discontinuous subbottom echoes; channel walls or levees: either eroded or aggrading internal reflectors; channels: 2–8 km wide, 7–15 m deep, downslope decrease in relief	Lower slopes of the northern Oki Bank and volcanic islands and seamounts, and the escarpment of the South Korea Plateau	Mass-flow chutes and channels (Flood and Damuth, 1987; Clark and Pickering, 1996)
	IV-3		Large-scale, slightly to strongly channelized surface topography with various bottom and subbottom echoes; 1.5–13.6 km wide, 15–85 m deep; asymmetric flank geometry in cross section; split into several branches in the southern part; channel floor: sharp to very prolonged bottom echoes with either no or a few intermittent, prolonged subbottom reflectors that are often truncated by the present channel-floor surface; channel margins or walls: slightly irregular topographic, indistinct bottom echoes which truncate distinct to indistinct internal reflectors; in the southern branches, local draping of small-scale, thin transparent layers on the channel floor	Axis of the Ulleung Interplain Gap	Bottom-current channel system (Johnson and Damuth, 1979; Johnson, 1984)

Echo types I-2, II-2, III-1 and IV-1 are modified from Lee et al. (2002).

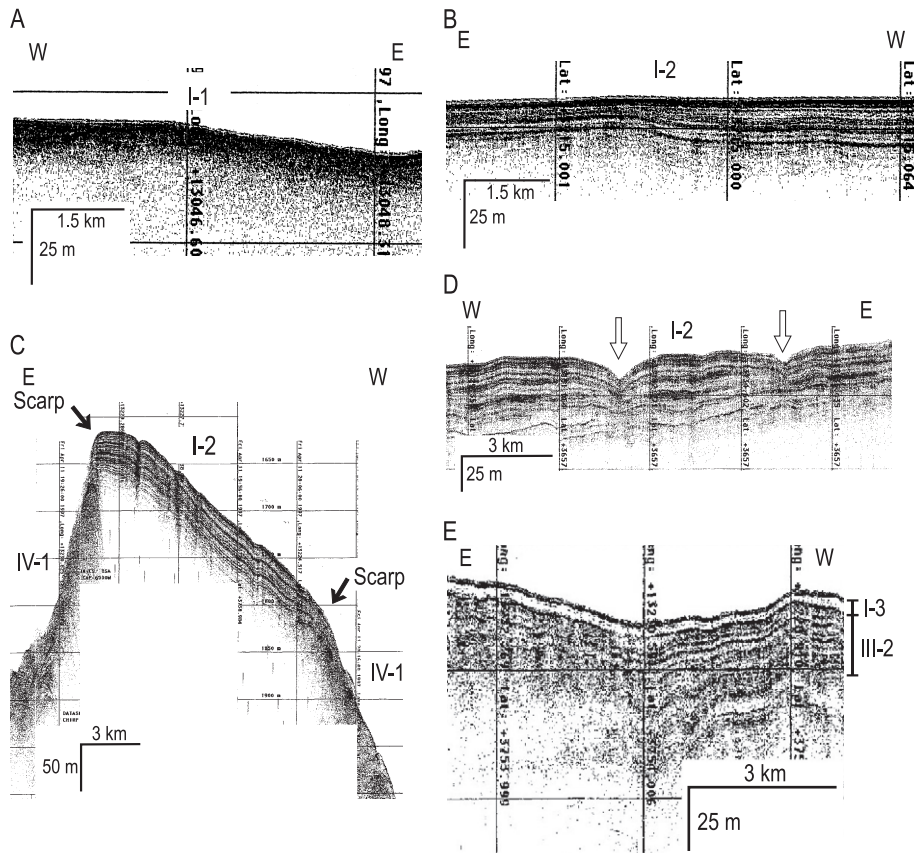


Fig. 5. High-resolution (2–7 kHz) subbottom profiles of distinct echoes (I). For location of each profile, see Fig. 1B. (A) Very sharp bottom echoes with either no or rare intermittent, discontinuous internal reflectors (type I-1). (B and C) Distinct bottom echoes and several continuous, parallel internal reflectors (type I-2) with either flat seafloor topography in the basin plain (B) or steeply inclined seafloor topography in the topographic highs (C). Note a dissection of type I-2 by scarps in (C). (D) Type I-2 containing small-scale, intermittent channel-levee systems (open arrows) in the basin plain. Note continuous aggrading internal reflectors in the levees. (E) An uppermost transparent (3–6 m thick) layer (type I-3) that is discordant to internal reflectors of the underlying sedimentary sequences (type III-2).

### 6.3. Northern basin plain of the Ulleung Basin

The northern basin plain consists dominantly of types I-2 and II-1 (turbidites) (Fig. 10). Types I-2 and II-1 contain a few small-scale, intermittent channel-levee systems (Figs. 5D and 6B). The channels are 0.3–1 km wide and <10 m deep. The channel-levee systems trend N–S or NNW–SSE (Fig. 10, open arrows), and decrease northward in channel relief. The systems often display lobate geometry in cross section (Fig. 6B). The lobate systems are generally stacked in topographically low areas of the underlying systems. The levees show continuous aggrading reflectors (Figs. 5D and 6B). Type I-2 (turbidites) is

often truncated by type IV-3 (large-scale, bottom-current channel system) (Fig. 9D). In core sediments, types I-2 and II-1 comprise dominant fine-grained turbidite sequences (facies LS, LM and HM) of Unit II and pelagic/hemipelagic succession (facies BM) of Unit I (Fig. 4).

### 6.4. Oki Bank, and Dok Island, Dok and Oki seamounts, and Ulleung Interplain Gap

The upper to middle slopes of the Dok and Oki seamounts and Dok Island are dominated by type III-1 (basement highs or outcrops) (Fig. 10). On the upper slope and ridge summits of the Oki Bank, type I-2

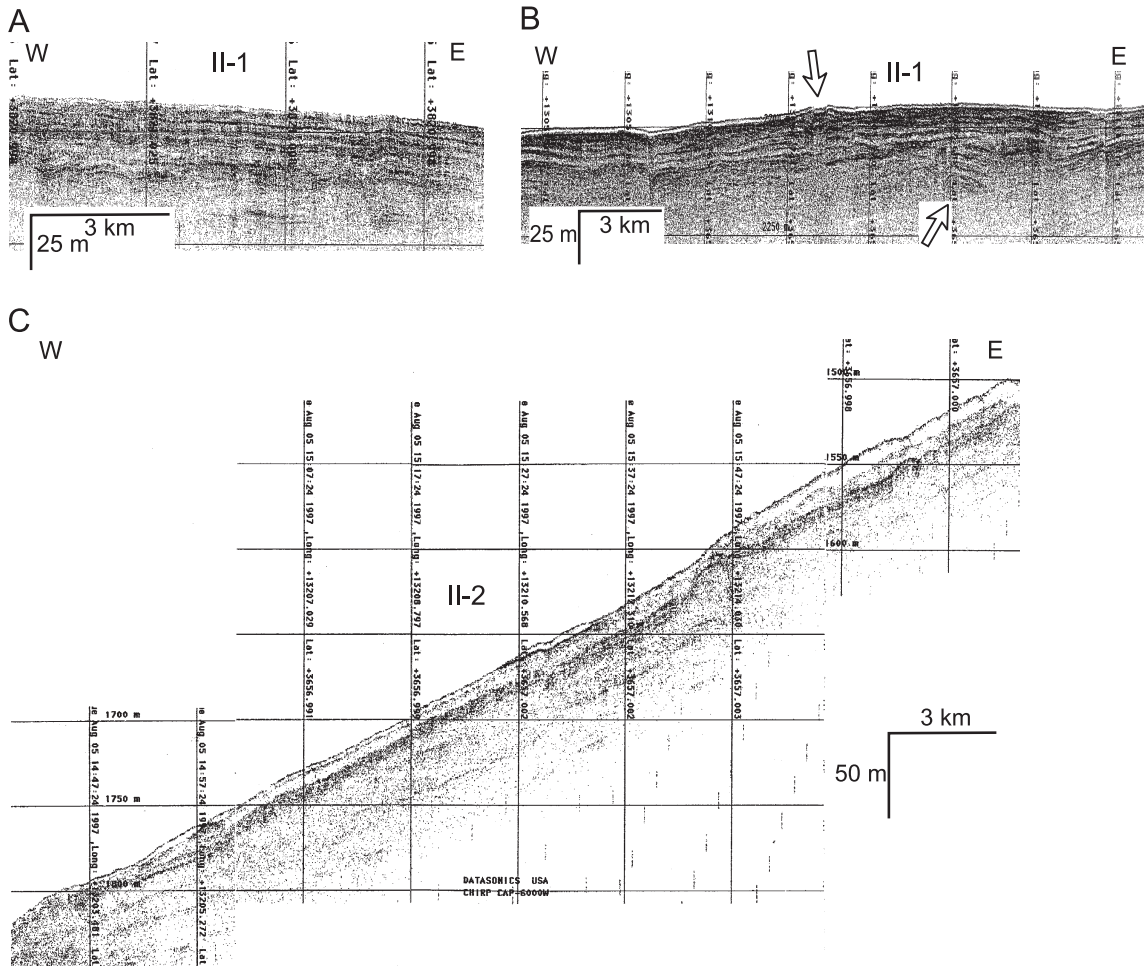


Fig. 6. Chirp (2–7 kHz) subbottom profiles of indistinct echoes (II). For location of each profile, see Fig. 1B. (A) Indistinct bottom echoes with either no or a few sub-parallel, intermittent internal reflectors (type II-1). (B) Type II-1 showing small-scale, intermittent channel-levee systems (open arrows). Note a lobate geometry of the channel-levee systems in cross section. (C) Laterally wedged, transparent masses (type II-2) in downslope-parallel section.

(pelagites/hemipelagites) occurs (Fig. 10). Type I-2 (pelagites/hemipelagites) is generally truncated by scarps or scars with a relief of a few metres to 90 m (Fig. 8A). Below the headwall scarp, several subsidiary scarps frequently occur. Regions of the headwall scarps are marked either by a glide/slide plane underlain by undisturbed to slightly disturbed sediments or by irregular drapes of small-scale, thin blocky, hyperbolic or transparent masses (Fig. 8A). Along the entire middle to lower slopes of the Oki Bank, Dok Island, and Dok and Oki seamounts, slides and slumps (type IV-1) are present below the headwall scarps (Fig. 10).

The scarps with displaced masses often exhibit step-like geometry.

Type IV-1 (slides and slumps) is transitional downslope to types II-2 (debrites), III-2 (fine-grained turbidity-current sediment waves) and IV-2 (mass-flow chutes/channels) (Fig. 10). Type II-2 (debrites) generally occurs as several stacks of sheet-like, shingled unit (Fig. 6C). Type IV-2 (mass-flow chutes/channels) is 4.5–8 km wide and less than 15 m deep. Chute or channel relief generally decreases downslope. The chutes and channels (type IV-2) are often extended into the Ulleung Interplain Channel (Fig. 10). In the

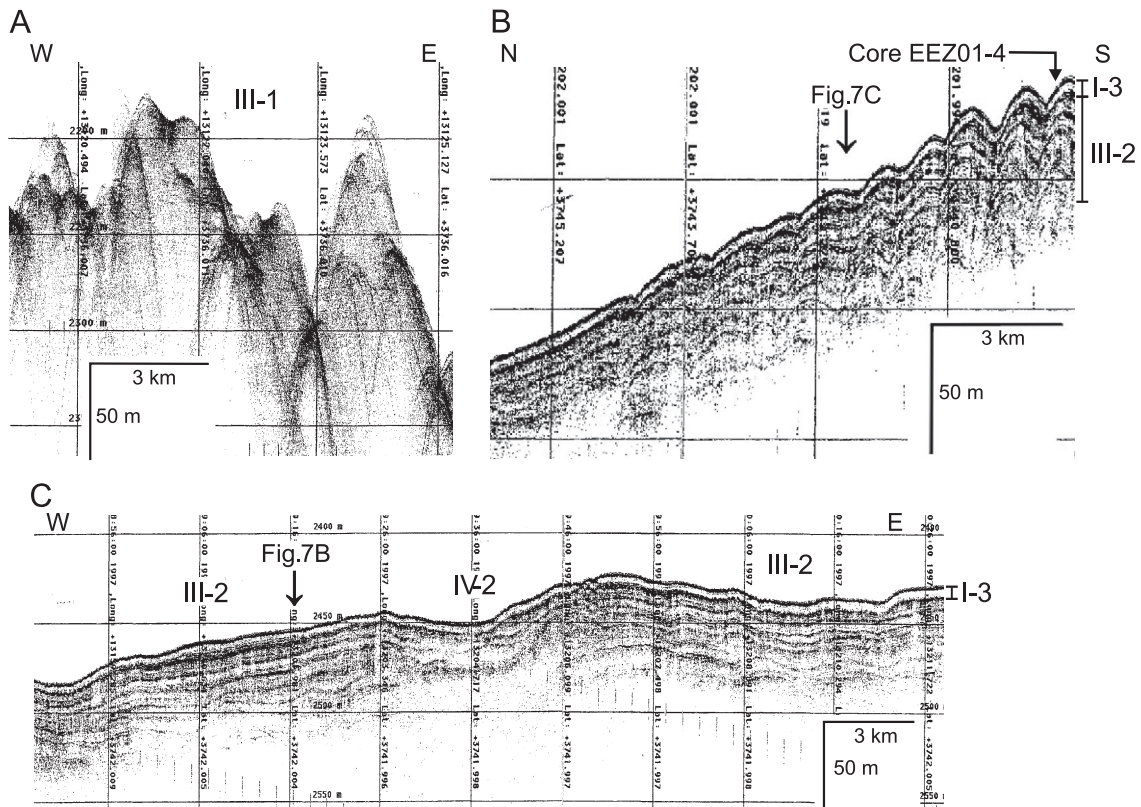


Fig. 7. High-resolution (2–7 kHz) subbottom profiles of hyperbolic or wavy echoes (III). For location of each profile, see Fig. 1B. (A) Large single or irregular overlapping hyperbolae with widely varying vertex elevation (type III-1). (B and C) Regular to slightly irregular wavy bottom echoes with upslope migrating internal reflectors (type III-2) in downslope- (B) and contour-parallel (C) sections. Note progressive downslope decrease in height and asymmetry of the waves, with steeper, thicker upslope and gentler, thinner downslope flanks in downslope-parallel section (B). Type III-2 is commonly overlain by an uppermost transparent layer (type I-3).

upslope area, chute and channel floor consists mostly of strongly convex-up, small-scale hummocky surface echoes with transparent subbottom echoes which gradually change downslope to slightly convex-up or nearly flat surface echoes with either transparent or a few discontinuous subbottom echoes. Type III-2 (fine-grained turbidity-current sediment waves) occurs along the entire lower slopes of the Oki Bank and Dok Island (Fig. 10). In core sediments, type III-2 corresponds to Unit II consisting dominantly of fine-grained turbidites (facies LS, LM and HM) interbedded with 'background' pelagic/hemipelagic muds (facies BM and CLM) (Fig. 4). Toward both up- and downslope, proportions of turbidite beds (facies LS, LM and HM) in type III-2 decrease (Fig. 4). The mass-flow deposits (types II-2 and III-2) in the lower

slope of the Oki Bank generally thin downslope, forming a large-scale, convex-up or mound morphology (Fig. 9).

In the northwestern lower slope of the Oki Bank, types III-2, II-2 and IV-2 (fine-grained turbidity-current sediment waves, debrites, and mass-flow chutes/channels) are overlain by type I-3 (bottom-current deposits) (Figs. 7B,C, 9C and 10). Type I-3 corresponds to a 3–4.2-m-thick succession (Unit I), mostly comprising muddy (facies BM) and manganiferous (facies ILM) contourites (Fig. 4). The lower part of type I-3 is dominated by manganiferous contourites (facies ILM) overlying the laminated Mn-carbonate mud (facies CaM) layer (Fig. 4). In the area of type I-3, Unit I is generally thicker than that in the Ulleung Interplain Channel and basin plain of the Ulleung

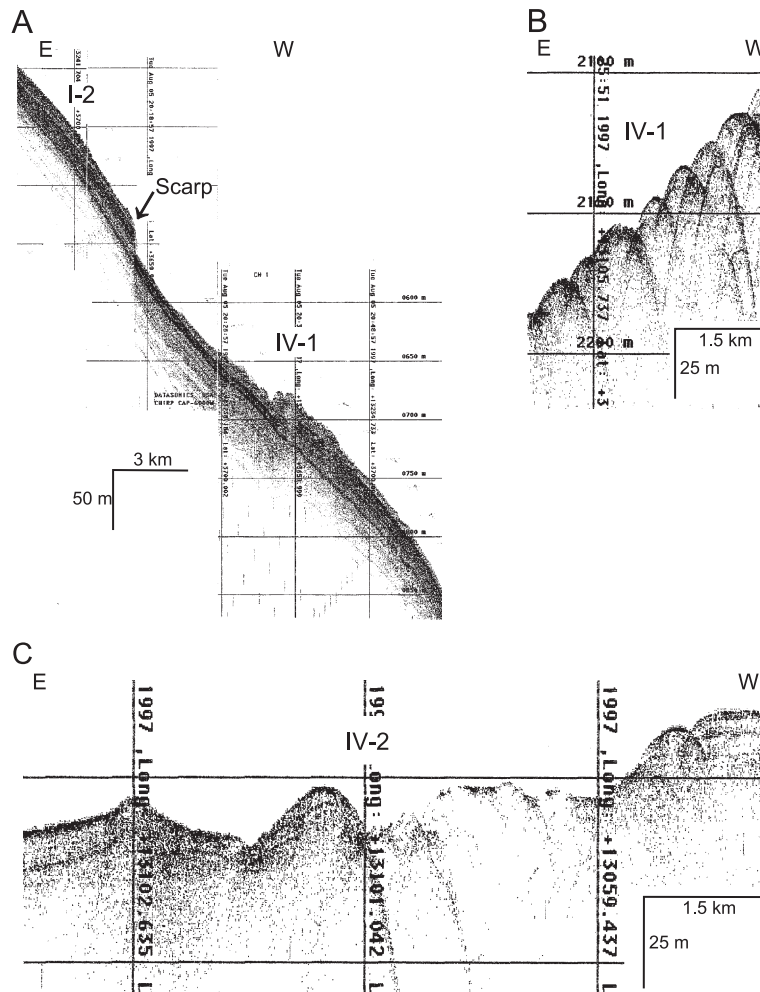


Fig. 8. Chirp (2–7 kHz) subbottom profiles of combined echoes (IV). For location of each profile, see Fig. 1B. (A) Irregular blocky, lumpy or hyperbolic masses bounded upslope by scars and scarps (type IV-1). (B) Local occurrence of strongly reflective, regular overlapping hyperbolae with slightly varying vertex elevation in type IV-1. (C) Channelized topography with various bottom and subbottom echoes (type IV-2).

Basin. In both high-resolution subbottom profiles and core sediments, type I-3 progressively thins, forming an elongate mound along the Ulleung Interplain Channel (Figs. 4 and 11).

The Ulleung Interplain Channel (UIC) is characterized by type IV-3 (large-scale bottom-current channel system) (Figs. 9 and 10). The channelized geometry is 1.5–13.6 km wide and 15–85 m deep. It is asymmetric in cross section: steep on the northwestern side (South Korea Plateau) and gentle on the southeastern side (Okii Bank and Dok Island) (Figs.

9A–C and 12). Near the North Ulleung Interplain Seamount (NUIS), the channel is relatively shallow (<20 m deep) (Figs. 9A and 12). To the south of the NUIS, it deepens southwestward, up to 85 m deep (Figs. 9B,C and 12). Near the Ulleung Seamount, it abruptly narrows and is split into several branches immediately south of the Ulleung Seamount (Figs. 9D, 10 and 12). These branches gradually shallow southward, but the easternmost branch extends to 36°50'N along the western base-of-slope of the Dok Island (Fig. 10).

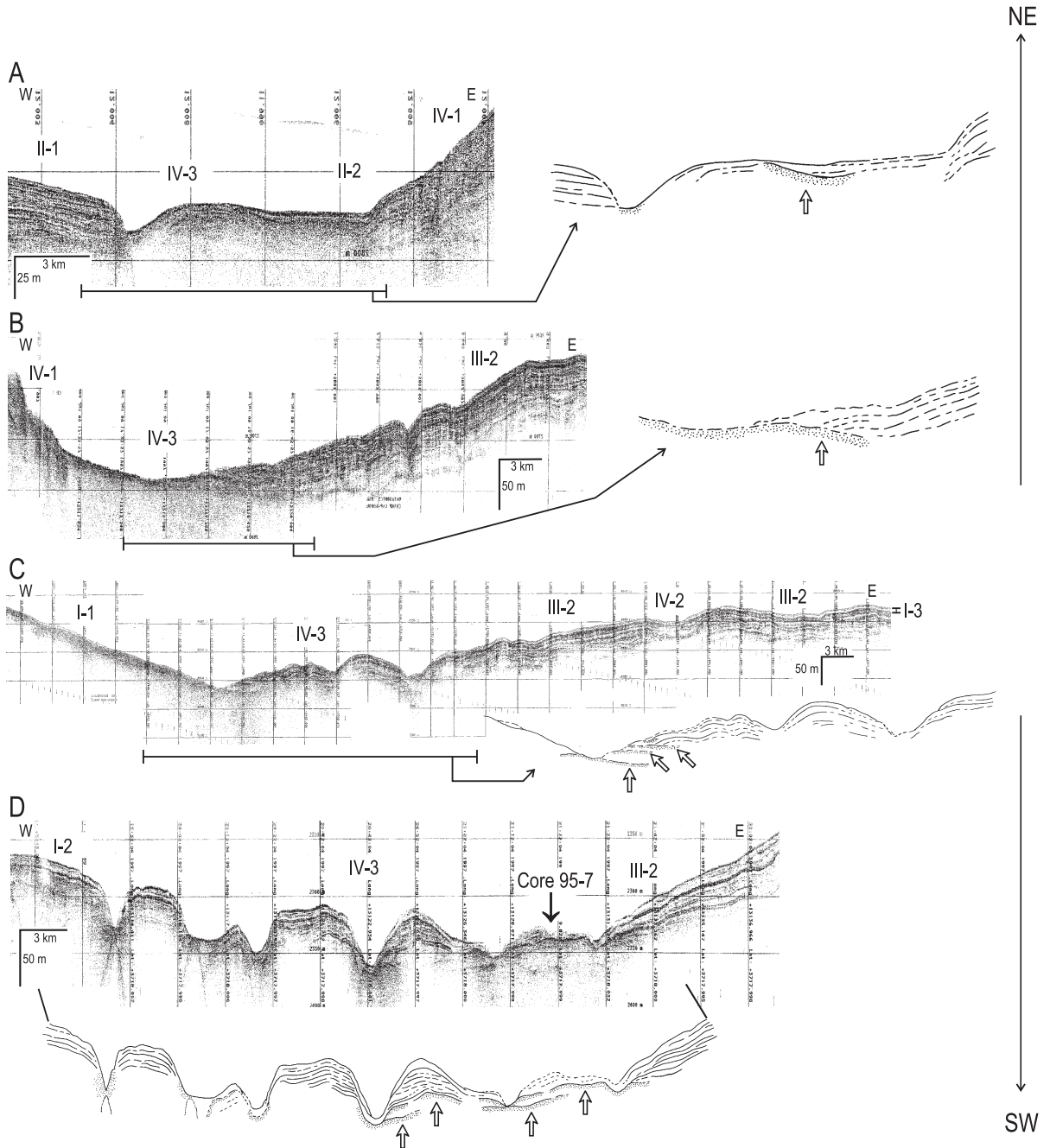


Fig. 9. High-resolution (2–7 kHz) subbottom profiles and line drawings of the Ulleung Interplain Channel (type IV-3) and the adjacent areas. For location of each profile, see Fig. 1B. Open arrows indicate prolonged subbottom reflectors with irregular topography in the floor of the Ulleung Interplain Channel.



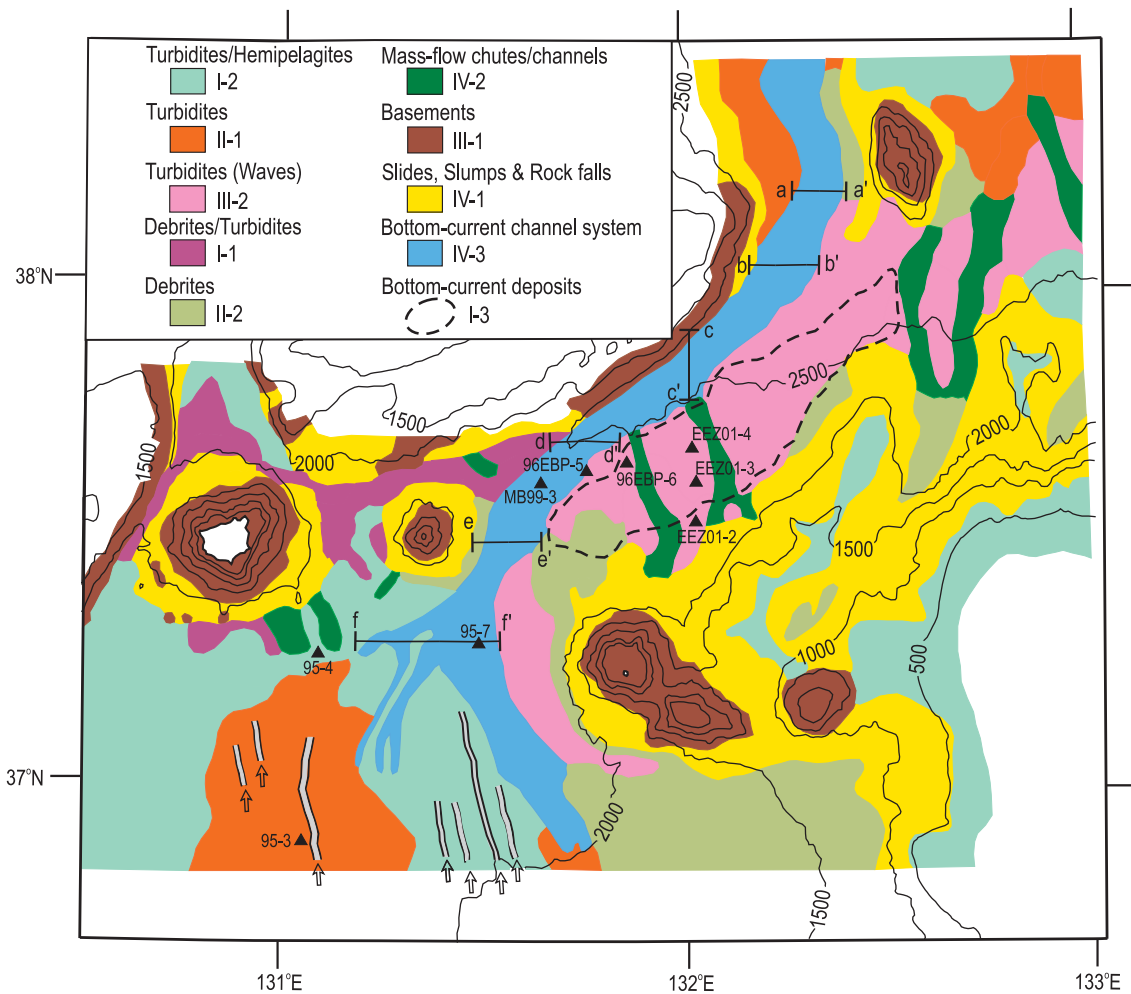


Fig. 10. Distribution of echo types and sedimentary processes in the Ulleung Interplain Gap and the adjacent areas. Triangles represent location of piston cores. Open arrows indicate small-scale, intermittent channel-levee systems in turbidites (types I-2 and II-1).

The UIC floor shows sharp to prolonged bottom echoes with either no or a few intermittent, prolonged internal reflectors (Fig. 9A–C). In this area, core sediments (core MB99-3) mostly comprise manganiferous (facies ILM) and muddy (facies BM) contourites which are interrupted by medium- to thick-bedded, coarse-grained, volcanoclastic turbidites (facies MGS) with thin-bedded, fine-grained turbidites (facies LS, LM and HM) (Fig. 4). In the southern branches, small-scale, irregular transparent masses partly drape the channel floor (Fig. 9D) in which core sediments (core 95-7) consist dominantly of muddy (facies BM) and manganiferous (facies ILM) contourites,

interbedded with a few fine-grained turbidites (facies BSM, LM and HM) (Fig. 4). The prolonged subsurface echoes in the channel floor are often truncated by the present channel-floor surface, and are overlapped by prograding masses of types II-2 and III-2 (Fig. 9, open arrows).

In the UIC walls, distinct to indistinct internal reflectors are generally truncated, showing slightly irregular topography (Fig. 9B,C). These internal reflectors generally display similar acoustic and geometric characters to type III-2, and commonly prograde towards the channel floor, downlapping onto the very prolonged subsurface echoes (Fig. 9B,C). In

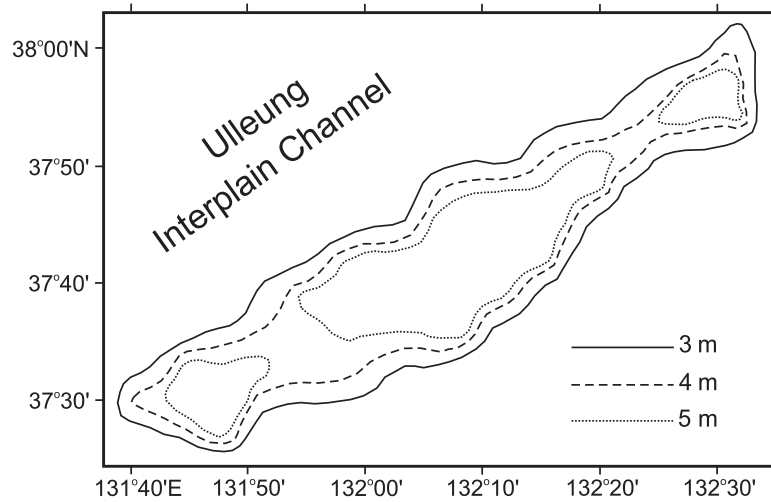


Fig. 11. Map showing thickness of an uppermost transparent layer (type I-3). Note an elongate, mound distribution along the Ulleung Interplain Channel.

the UIC walls, core sediments (core 95EBP-5) dominantly comprise muddy (facies BM) and manganiferous (facies ILM) contourites, interbedded with fine-grained turbidites (facies LS, LM and HM) (Fig. 4). Unit I in the UIC is generally thinner than that in the lower slope of the Oki Bank and the northern basin plain of the Ulleung Basin. The CaM layers only occur in the UIC below the anoxic intervals of the last glacial maximum period (Fig. 4), implying an overall reduction of sedimentation rate in the UIC region.

## 7. Discussion

Along the entire slopes of topographic highs around the Ulleung Interplain Gap (UIG), extensive occurrence of mass-movement and mass-flow deposits reflects frequent slope failures. In core sediments from the lower slope of the Oki Bank, fine-grained turbidites are dominant in Unit II (> ~ 15 ka), suggesting that slope failures frequently occurred with recurrence intervals of ca. 250–500 years (upper Unit II, ca. 15–24.7 ka) during the last-glacial

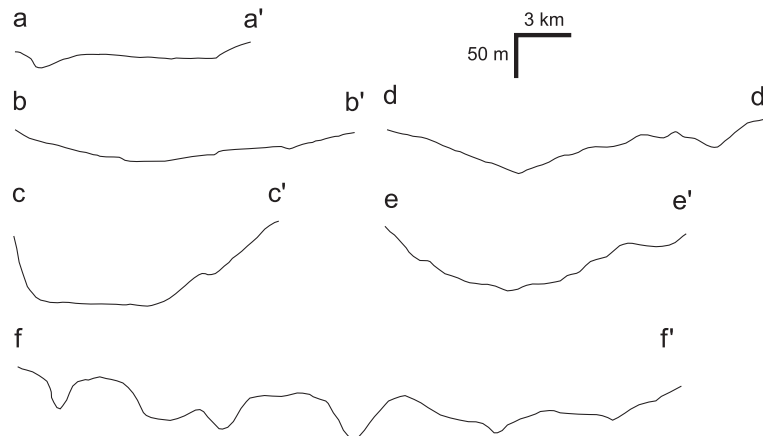


Fig. 12. Cross-sectional geometry of the Ulleung Interplain Channel. For location of each section, see Fig. 10.

period when sea level was lowered (Fig. 13B). The mass-movement and mass-flow deposits display a distinctive zonal distribution (Fig. 10); slides, slumps and rock falls occur on the upper to middle slopes, and mass-flow chutes/channels, debrites and turbidites on the base-of-slope and distal part of the lower slope. The distinctive zonal distribution reflects that the slope failures were initiated at the upper to

middle slopes of the topographic highs and evolved successively downslope into debris flows and turbidity currents (Fig. 13B; e.g., Chough et al., 1997; Lee et al., 2002). The several subsidiary scarps below the headwall scarp and the step-like geometry of failed mass with scarps indicate retrogressive slope failures (e.g., Mulder and Cochonat, 1996; Chough et al., 1997).

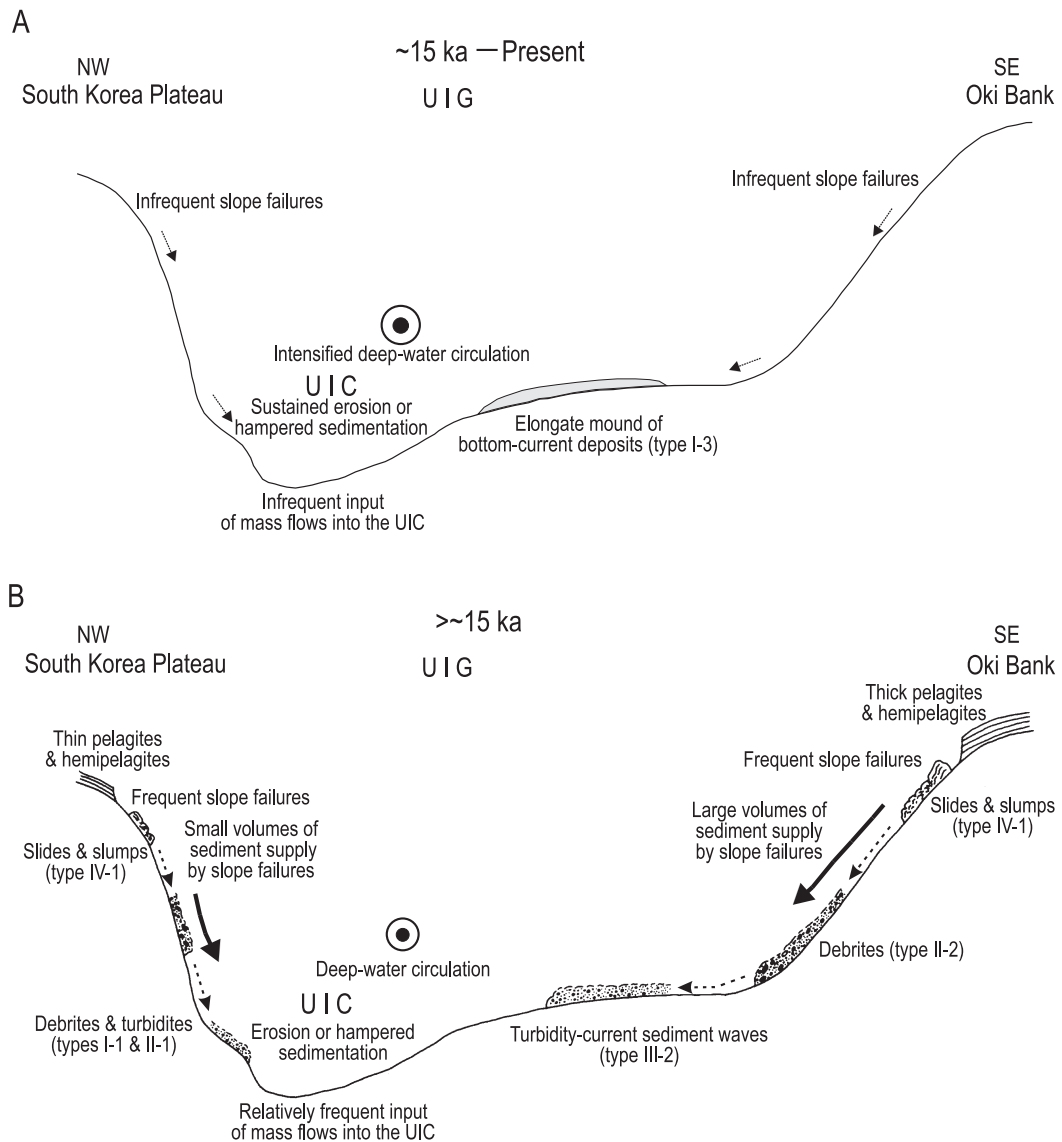


Fig. 13. Schematic diagrams of the depositional model in the Ulleung Interplain Gap and the adjacent areas during the late Quaternary. Cross sections cut through the South Korea Plateau and the Oki Bank. UIC = Ulleung Interplain Channel; UIG = Ulleung Interplain Gap.

The extensive slope failures and mass-flow deposits on the entire slopes of topographic highs around the UIG suggest that a relatively large amount of sediment was delivered from the topographic highs into the UIG by downslope gravitational processes (Fig. 13B). However, the pattern of sediment supply was asymmetrical. A relatively large amount of sediment was supplied from the wide areas of large-scale slope failures along the entire slopes of the Oki Bank and Dok Island (Figs. 10 and 13B). The mass flows prograded into the UIG, forming a large-scale, gentle convex-up or mound morphology of turbidity-current sediment waves and debrites on the southeastern UIG (Figs. 9B,C and 13B). In contrast, a relatively small volume of sediment was transported into the UIG from the escarpment of the South Korea Plateau and formed a narrow, steep geometry of mass-flow deposits on the northwestern UIG (Figs. 9B,C and 13B).

The truncated reflectors of channel walls, the muddy (BM) and manganiferous (ILM) contourites, and the occurrence of type IV-3 along the UIG axis are indicative of erosion or hampered sedimentation in the Ulleung Interplain Channel (UIC) by bottom currents (Fig. 13; e.g., Johnson and Damuth, 1979; Johnson, 1984; Chough et al., 1985; Stow et al., 1998). Southwestward-flowing bottom currents in the UIG may have decreased in flow strength or velocity at the downcurrent exit, immediately south of the Ulleung Seamount, due to the flow expansion, resulting in channel branching in the southern UIC and the southward shallowing of channel relief (Figs. 9D and 10). The southeastern UIC flank is characterized by a large-scale, gentle mound morphology of mass-flow deposits derived from the slopes of the Oki Bank and Dok Island (Figs. 9B,C and 10). The large-scale, gentle mound geometry of mass-flow deposits on the southeastern UIC flank reflects that most of the sediments supplied by downslope gravitational processes were not removed by alongslope bottom currents (Fig. 13B). In contrast, a narrow, steep morphology of mass-flow deposits on the northwestern UIC flank may be attributed to a relatively small amount of sediment input by downslope gravitational processes from the slopes of the South Korea Plateau (Fig. 13B).

Mass flows derived from the slopes of the Oki Bank and Dok Island prograded towards the UIC, downlapping onto the concave-up, very prolonged

subbottom subsurface echoes in the channel floor (Fig. 9B,C). Bottom currents have probably eroded the most distal part of the prograding mass-flow deposits, forming an incised-channel geometry (Fig. 13). These features suggest that the relief of the southeastern UIC margin has been maintained by combination of bottom-current and mass-flow activities. Some large-scale mass flows derived from the topographic highs around the UIG may have intermittently entered into the topographically low areas of the UIC, resulting in the interbedded coarse- or fine-grained turbidites (facies MGS, LS, LM and HM) (Figs. 4 and 13). In core sediments from the southern UIC flank (i.e., northwestern lower slope of the Oki Bank), the dominant manganiferous contourites (ILM) directly above the CaM layer (i.e., boundary between Units I and II) and rare turbidites in Unit I (< ~ 15 ka) reflect intensified deep-water circulation and infrequent slope failures (recurrence intervals of ca. 1700–5000 years) in the UIG after sea-level rise at ~ 15 ka (Fig. 13A). Under these conditions, a thin, elongate mound of bottom-current drifts (type I-3, succession of muddy and manganiferous contourites) overlying mass-flow deposits (types II-2 and III-2) on the southeast flank of the UIC was formed, and erosion or hampered sedimentation continued in the UIC (Fig. 13A).

In the UIG, the sediment waves (type III-2) on the southeastern flank of the UIC are apparently similar to bottom-current wavy drifts on channel flanks in other deep passages, e.g., Vema Channel and São Paulo Abyssal Gap (Johnson, 1984; Faugères et al., 1998) and Amirante Passage (Johnson and Damuth, 1979; Johnson et al., 1983). Wave crests of bottom-current drifts are generally perpendicular or oblique to principal bottom-current direction (Flood and Shor, 1988; Faugères et al., 1998; Wynn and Stow, 2002). However, wave crests on the southeastern flank of the UIC are aligned parallel to the NE–SW-trending regional slope which is parallel to the SW-flowing bottom current direction in the UIG. In addition, the sediment waves (type III-2) decrease downslope in wave height, thickness of layers and wave asymmetry (Fig. 7B), and comprise fine-grained turbidites (LS, LM and HM) interbedded with ‘background’ pelagic/hemipelagic sediments (BM and CLM) (Fig. 4). These sedimentary features reflect that the wavy sediments were most likely generated by turbidity currents

derived from the slopes of the Oki Bank and Dok Islands, rather than channel-related drifts formed by bottom currents (e.g., Wynn et al., 2000b; Wynn and Stow, 2002).

Immediately south of the UIC branches, small-scale channel-levee systems (types I-2 and II-1) occur intermittently (Fig. 10). The channel-levee systems south of the UIC are not connected with the branches of the UIC, and exhibit a non-radial pattern (i.e., consistent N–S or NNW–SSE orientation) (Fig. 10) and a northward decrease in channel relief, opposite to the southward shallowing of the UIC branches. Although the location of the channel-levee systems is similar to that of channel-lobe systems of contourite fans developed at the down-current exit of an axial bottom-current channel (Mézerai et al., 1993; Faugères et al., 1998), these features reflect that the channel-levee systems are not related to the UIC system. The extensive occurrence of large-scale slope failures, debrites and turbidites on the southern margin of the Ulleung Basin (Chough et al., 1985; Lee et al., 1999) and the northward reduction in channel relief suggest that the channel-levee systems were intermittently formed by turbidity currents derived from the southern margin of the Ulleung Basin.

Hydrography in deep-water passages generally shows that bottom currents are spatially variable in intensity (Johnson and Damuth, 1979; Hogg et al., 1982; Hogg, 1983). Spatial variation in bottom-current intensity controls the sedimentation pattern of the axial channel, channel flanks and channel exit (Johnson and Damuth, 1979; Johnson et al., 1983; Johnson, 1984; Mézerai et al., 1993). In the area of relatively weak bottom currents, a wide, gentle channel flank with sediment waves occurs. In contrast, a narrow, steep channel flank forms in the area of relative strong bottom currents. This spatial variation in bottom-current intensity causes an asymmetric channel-margin geometry in cross section (Johnson and Damuth, 1979; Johnson, 1984). In addition, channel-lobe systems of contourite fans commonly form at the exit of an axial channel where bottom-current strength diminishes (Mézerai et al., 1993; Faugères et al., 1998). Like other deep passages, the UIG has an axial channel system (UIC) with asymmetric channel-flank geometry, channel-levee systems at its downcurrent exit, and sediment

waves on the flank. Without a detailed analysis, these sedimentary features can be easily misinterpreted in terms of spatial variation in bottom-current activity. However, the sedimentary features in the UIG were influenced by an interaction between bottom currents and mass flows.

## 8. Conclusions

A synthesis of high-resolution subbottom profiles and long sediment cores from the Ulleung Interplain Gap (UIG) and the adjacent areas reveals that sedimentary processes in the deep passage were dominated by an interaction between bottom currents and mass flows during the last- and post-glacial periods.

During the last-glacial period ( $> \sim 15$  ka) when sea level was lowered, a relatively large amount of sediment was derived from the surrounding topographic highs into the UIG by frequent mass flows (recurrence intervals of ca. 250–500 years in the upper Unit II). Southwestward-flowing bottom currents caused erosion or hampered sedimentation in the Ulleung Interplain Channel (UIC), and formed the UIC branches at the southern exit of the UIG. Large-scale mass flows derived from the slopes of the Oki Bank formed a large, gentle mound morphology of turbidity-current sediment waves and debrites on the southeastern UIC flank, overwhelming alongslope bottom currents. In contrast, a narrow, steep geometry of mass-flow deposits on the northwestern UIC flank was ascribed to a small amount of sediment supplied from the slopes of the South Korea Plateau.

In post-glacial time ( $< \sim 15$  ka), intensified bottom-current activity and infrequent slope failures (recurrence intervals of 1700–5000 years) formed a thin, elongate mound of bottom-current drifts overlying mass-flow deposits on the southeastern UIC flank, and sustained erosion or hampered deposition in the UIC.

Unlike other deep passages where sedimentary features are mostly formed by bottom currents, the UIG was under influence of both alongslope bottom currents and downslope gravitational processes, forming the asymmetric cross-sectional geometry of the UIC flanks, sediment waves on the southeastern UIC

flank, and intermittent channel-levee systems at the downcurrent exit of the UIG.

## Acknowledgements

This research was supported to Chough by grant nos. R03-2001-00037 and 2003-16 of the Korea Science and Engineering Foundation (KOSEF) and BK21 Project (Ministry of Education and Human Resources), and to Lee by Post-doctoral Fellowship Program of the KOSEF. Bahk was supported by the Korea Ocean Research and Development Institute under grant PE87500. We are grateful to the Regional Seafloor Mapping Division of the National Oceanographic Research Institute of Korea for providing Chirp subbottom profiles. We also thank Drs. Howe, Lebreiro and Piper for useful and constructive comments on the manuscript.

## References

- Armishaw, J.F., Holmes, R.W., Stow, D.A.V., 1998. Morphology and sedimentation on the Hebrides Slope and Barra Fan, NW UK continental margin. In: Stoker, M.S., Evans, D., Cramp, A. (Eds.), *Geological Processes on Continental Margins: Sedimentation, Mass-Wasting and Stability*. Geol. Soc. London Spec. Publ., vol. 41, pp. 81–104.
- Bahk, J.J., Chough, S.K., Han, S.J., 2000. Origins and paleoceanographic significance of laminated muds from the Ulleung Basin, East Sea (Sea of Japan). *Mar. Geol.* 162, 459–477.
- Bahk, J.J., Chough, S.K., Jeong, K.S., Han, S.J., 2001. Sedimentary records of paleoenvironmental changes during the last deglaciation in the Ulleung Interplain Gap, East Sea (Sea of Japan). *Glob. Planet. Change* 28, 241–253.
- Bouma, A.H., 1962. *Sedimentology of Some Flysch Deposits*. Elsevier, Amsterdam.
- Carter, L., 2001. A large submarine debris flow in the path of the Pacific deep western boundary current off New Zealand. *Geo Mar. Lett.* 21, 42–50.
- Carter, L., McCave, I.N., 1997. The sedimentary regime beneath the deep western boundary current Inflow to the southwest Pacific Ocean. *J. Sed. Res.* 67, 1005–1017.
- Chang, K.I., Hogg, N.G., Suk, M.S., Byun, S.K., Kim, K., 2002. Mean flow and variability in the southwestern East Sea. *Deep-Sea Res.* 49, 2261–2279.
- Chough, S.K., Jeong, K.S., Honza, E., 1985. Zoned facies of mass-flow deposits in the Ulleung (Tsushima) Basin, East Sea (Sea of Japan). *Mar. Geol.* 65, 113–125.
- Chough, S.K., Lee, S.H., Kim, J.W., Park, S.C., Yoo, D.G., Han, H.S., Yoon, S.H., Oh, S.B., Kim, Y.B., Back, G.G., 1997. Chirp (2–7 kHz) echo characters in the Ulleung Basin. *Geosci. J.* 1, 143–153.
- Chough, S.K., Lee, H.J., Yoon, S.H., 2000. *Marine Geology of Korean Seas*, 2nd edn. Elsevier, Amsterdam.
- Clark, J.D., Pickering, K.T., 1996. *Submarine Channels: Processes and Architecture*. Vallis Press, London.
- Crusius, J., Pedersen, T.F., Calvert, S.E., Cowie, G.L., Oba, T., 1999. A 36 kyr geochemical record from the Sea of Japan of organic matter flux variations and changes in intermediate water oxygen concentrations. *Paleoceanography* 14, 248–259.
- Damuth, J.E., 1980. Use of high-frequency (3.5–12 kHz) echograms in the study of near-bottom sedimentation processes in the deep-sea: a review. *Mar. Geol.* 38, 51–75.
- Embley, R.W., 1976. New evidence for occurrence of debris flow deposits in the deep sea. *Geology* 4, 371–374.
- Embley, R.W., Jacobi, R.D., 1977. Distribution and morphology of large submarine sediment slides and slumps on Atlantic continental margins. *Mar. Geotechnol.* 2, 205–228.
- Faugères, J.C., Mézerais, M.L., Stow, D.A.W., 1993. Contourite drift types and their distribution in the North and South Atlantic Ocean basins. *Sediment. Geol.* 82, 189–203.
- Faugères, J.C., Imbert, P., Mézerais, M.L., Crémer, M., 1998. Seismic patterns of a muddy contourite fan (Vema Channel, South Brazilian Basin) and a sandy distal turbidite deep-sea fan (Cap Ferret system, Bay of Biscay): a comparison. *Sed. Geol.* 115, 81–110.
- Faugères, J.C., Stow, D.A.V., Imbert, P., Viana, A., 1999. Seismic features diagnostic of contourite drifts. *Mar. Geol.* 162, 1–38.
- Flood, R.D., Damuth, J.E., 1987. Quantitative characteristics of sinuous distributary channels on the Amazon Deep-Sea Fan. *Bull. Geol. Soc. Am.* 98, 728–738.
- Flood, R.D., Shor, A.N., 1988. Mud waves in the Argentine Basin and their relationship to regional bottom circulation patterns. *Deep-Sea Res.* 35, 943–971.
- Gamo, T., 1999. Global warming may have slowed down the deep conveyor belt of a marginal sea of the northwestern Pacific: Japan Sea. *Geophys. Res. Lett.* 26, 3141–3144.
- Gamo, T., Horibe, Y., 1983. Abyssal circulation in the Japan Sea. *J. Oceanogr. Soc., Japan* 39, 220–230.
- Gamo, T., Nozaki, Y., Sakai, H., Nakai, T., Tsubota, H., 1986. Spatial and temporal variations of water characteristics in the Japan Sea bottom layer. *J. Mar. Res.* 44, 781–793.
- Gorbarenko, S.A., Southon, J.R., 2000. Detailed Japan Sea paleoceanography during the last 25 kyr: constraints from AMS dating and  $\delta^{18}\text{O}$  of planktonic foraminifera. *Paleogeogr. Paleoclimatol. Paleoecol.* 156, 177–193.
- Hogg, N.G., 1983. Hydraulic control and flow separation in a multi-layered fluid with applications to the Vema Channel. *J. Phys. Oceanogr.* 13, 695–708.
- Hogg, N.G., Biscaye, P., Gardner, W., Schmitz Jr., W.J. 1982. On the transport and modification of Antarctic bottom water in the Vema Channel. *J. Mar. Res.* 40, 231–263 (supplement).
- Hollister, C.D., Johnson, D.A., Lonsdale, P.F., 1974. Current-controlled abyssal sedimentation: Samoan Passage, equatorial west Pacific. *J. Geol.* 82, 275–300.
- Howe, J.A., 1996. Turbidite and contourite sediment waves in the

- northern Rockall Trough, North Atlantic Ocean. *Sedimentology* 43, 219–234.
- Howe, J.A., Pudsey, C.J., 1999. Antarctic circumpolar deep water: a Quaternary paleoflow record from the northern Scotia Sea, south Atlantic Ocean. *J. Sediment. Res.* 69, 847–861.
- Howe, J.A., Pudsey, C.J., Cunningham, A.P., 1997. Pliocene–Holocene contourite deposition under the Antarctic circumpolar current, western Falkland Trough, south Atlantic Ocean. *Mar. Geol.* 138, 27–50.
- Johnson, D.A., 1984. The Vema Channel: physiography, structures, and sediment–current interactions. *Mar. Geol.* 58, 1–34.
- Johnson, D.A., Damuth, J.E., 1979. Deep thermohaline flow and current-controlled sedimentation in the Amirante Passage: western Indian Ocean. *Mar. Geol.* 33, 1–44.
- Johnson, D.A., Ledbetter, M.T., Damuth, J.E., 1983. Neogene sedimentation and erosion in the Amirante Passage, western Indian Ocean. *Deep-Sea Res.* 30, 195–219.
- Jolivet, L., Shibuya, H., Fournier, M., 1995. Paleomagnetic rotations and the Japan Sea opening. In: Taylor, B., Natland, J. (Eds.), *Active Margins and Marginal Basins of the Western Pacific*. AGU Geophys. Monogr., vol. 88, pp. 355–369.
- Kawamura, H., Wu, P., 1998. Formation mechanism of Japan Sea Proper Water in the flux center off Vladivostok. *J. Geophys. Res.* 103, 21611–21622.
- Keigwin, W.D., Gorbarenko, S.A., 1992. Sea level, surface salinity of the Japan Sea, and the Younger Dryas event in the northwestern Pacific Ocean. *Quat. Res.* 37, 346–360.
- Kim, K.-R., Kim, K., 1996. What is happening in the East Sea (Japan Sea): recent chemical observation during CREAMS 93–96. *J. Korean Soc. Oceanogr.* 31, 164–172.
- Kim, K., Kim, K.-R., Chung, J.-Y., Yoo, H.-S., Park, S.-G., 1991. Characteristics of physical properties in the Ulleung Basin. *J. Oceanol. Soc. Korea* 26, 83–100.
- Kim, K., Kim, Y.-G., Cho, Y.-K., Takematsu, M., Volkov, Y., 1999. Basin-to-basin and year-to-year variation of temperature and salinity characteristics in the East Sea (Sea of Japan). *J. Oceanogr.* 55, 103–109.
- Kim, K.R., Kim, G., Kim, K., Lobanov, V., Ponomarev, V., Salyuk, A., 2002. A sudden bottom-water formation during the severe winter 2000–2001: the case of the East/Japan Sea. *Geophys. Res. Lett.* 29, 751–754.
- Laine, E.P., Damuth, J.E., Jacobi, R., 1986. Surficial sedimentary processes revealed by echo-character mapping in the western North Atlantic Ocean. In: Vogt, P.R., Tucholke, B.E. (Eds.), *The Western North Atlantic Region*. GSA The Geology of North America, vol. M, GSA, Boulder, CO, pp. 427–436.
- LeBlanc, L.R., Mayer, L., Rufino, M., Schock, S.G., King, J., 1992. Marine sediment classification using the chirp sonar. *J. Acoust. Soc. Am.* 91, 107–115.
- Lee, S.H., 2001. Depositional Processes of Quaternary Sediments in the Ulleung Basin, South Korea Plateau, Ulleung Interplain Gap and Oki Bank, East Sea: Chirp (2–7 kHz) Profiles. PhD thesis. Seoul National University, Seoul.
- Lee, H.J., Chough, S.K., Yoon, S.H., 1996. Slope-stability change from late Pleistocene to Holocene in the Ulleung Basin, East Sea (Japan Sea). *Sediment. Geol.* 104, 39–51.
- Lee, S.H., Chough, S.K., Back, G.G., Kim, Y.B., Sung, B.S., 1999. Gradual downslope change in high-resolution acoustic characters and geometry of large-scale submarine debris lobes in Ulleung Basin, East Sea (Sea of Japan), Korea. *Geo Mar. Lett.* 19, 161–254.
- Lee, S.H., Chough, S.K., Back, G.G., Kim, Y.B., 2002. Chirp (2–7 kHz) echo characters of the South Korea Plateau: styles of mass movement and sediment gravity flow. *Mar. Geol.* 184, 227–247.
- Locker, S.D., Laine, P., 1992. Paleogene–Neogene depositional history of the middle US Atlantic continental rise: mixed turbidite and contourite depositional systems. *Mar. Geol.* 103, 137–164.
- Machida, H., 1999. The stratigraphy, chronology and distribution of distal marker-tephras in and around Japan. *Glob. Planet. Change* 21, 71–94.
- Massé, L., Faugères, J.C., Hrovatin, V., 1998. The interplay between turbidity and contour current processes on the Columbia Channel fan drift, Southern Brazil Basin. *Sed. Geol.* 115, 111–132.
- McCave, I.N., Carter, L., 1997. Recent sedimentation beneath the Deep Western Boundary Current off northern New Zealand. *Deep-Sea Res.* 44, 1203–1237.
- McMaster, R.L., Locker, S.D., Laine, E.P., 1989. The early Neogene continental rise off the eastern United States. *Mar. Geol.* 87, 123–137.
- Meinert, J., 1986. Akustratigraphie im äquatorialen Ostatlantik: Zur Entwicklung der Tiefenwasserzirkulation der letzten 3.5 Millionen Jahre. *Meteor-Forschungsergeb.* C40, 19–86.
- Mézerai, M.L., Faugères, J.C., Figueiredo Jr., A.G., Massé, L., 1993. Contour current accumulation off the Vema Channel mouth, southern Brazil Basin: pattern of a “contourite fan”. *Sediment. Geol.* 82, 173–187.
- Moriyasu, S., 1972. The Tsushima current. In: Stommel, H., Yoshida, K. (Eds.), *University of Washington Press, U.S.A., Kuroshio*, pp. 353–369.
- Mulder, T., Cochonat, P., 1996. Classification of offshore mass movements. *J. Sediment. Res.* 66, 43–57.
- Nardin, T.R., Hein, F.J., Gorsline, D.S., Edwards, B.D., 1979. A review of mass movement processes, sediment and acoustic characteristics in slope and base-of-slope systems versus canyon-fan-basin floor systems. In: Doyle, L.J., Pilkey, O.H. (Eds.), *Geology of Continental Slopes*. SEPM Spec. Publ., vol. 27, pp. 61–73.
- Nitsche, F.O., Cunningham, A.P., Larter, R.D., Gohl, K., 2000. Geometry and development of glacial continental margin depositional systems in the Bellingshausen Sea. *Mar. Geol.* 162, 277–302.
- Normark, W.R., Hess, G.R., Stow, D.A.V., Bowen, A.J., 1980. Sediment waves on the Monterey Fan levee: a preliminary physical interpretation. *Mar. Geol.* 37, 1–18.
- Oba, T., Kato, M., Kitazato, H., Koizumi, I., Omura, A., Sakai, T., Takayama, T., 1991. Paleoenvironmental changes in the Japan Sea during the last 85,000 years. *Paleoceanography* 6, 499–518.
- Piper, D.J.W., 1978. Turbidite muds and silts on deep sea fans and abyssal plains. In: Stanley, D.J., Kelling, G. (Eds.), *Sedimentation in Submarine Canyons, Fans, and Trenches*. Dowden, Hutchinson and Ross, Stroudsburg, PA, pp. 163–176.

- Rebesco, M., Larter, R.D., Camelenghi, A., Barker, P.F., 1996. Giant sediment drifts on the continental rise west of the Antarctic Peninsula. *Geo Mar. Lett.* 16, 65–75.
- Schock, S.G., LeBlanc, L.R., Mayer, L.A., 1989. Chirp subbottom profiler for quantitative sediment analysis. *Geophysics* 54, 445–450.
- Senju, T., Aramaki, T., Otosaka, S., Togawa, O., Danchenkow, M., Karasev, E., Volkov, Y., 2002. Renewal of the bottom water after the winter 2000–2001 may spin-up the thermohaline circulation in the Japan Sea. *Geophys. Res. Lett.* 29 531–534.
- Seung, Y.-H., Yoon, J.-H., 1995. Some features of winter convection in the Japan Sea. *J. Oceanogr.* 51, 61–73.
- Stoker, M.S., 1998. Sediment-drift development on the continental margin off NW Britain. In: Stoker, M.S., Evans, D., Cramp, A. (Eds.), *Geological Processes on Continental Margins: Sedimentation, Mass-Wasting and Stability*. *Geol. Soc. London Spec. Publ.*, vol. 129, pp. 229–254.
- Stow, D.A.V., Reading, H.G., Collison, J.D., 1996. Deep Seas. In: Reading, H.G. (Ed.), *Sedimentary Environments: Processes, Facies and Stratigraphy*. Blackwell, Oxford, pp. 395–453.
- Stow, D.A.W., Gaugeres, J.C., Viana, A., Gonthier, E., 1998. Fossil contourites: a critical review. *Sediment. Geol.* 115, 3–31.
- Tucholke, B.E., Mountain, G.S., 1986. Tertiary paleoceanography of the western North Atlantic Ocean. In: Vogt, P.R., Tucholke, B.E. (Eds.), *The Western North Atlantic Region. GSA The Geology of North America*, vol. M, GSA, Boulder, CO, pp. 631–650.
- Uda, M., 1934. The results of simultaneous oceanographical investigations in the Japan Sea and its adjacent waters in May and June, 1932. *J. Imp. Fish. Exp.* 5, 57–190 (in Japanese).
- Watanabe, Y.W., Watanabe, S., Tsunogai, S., 1991. Tritium in the Japan Sea and the renewal time of the Japan Sea deep water. *Mar. Chem.* 34, 97–108.
- Wynn, R.B., Stow, D.A.V., 2002. Classification and characterisation of deep-water sediment waves. *Mar. Geol.* 192, 7–22.
- Wynn, R.B., Masson, D.G., Stow, D.A.V., Weaver, P.E., 2000a. Turbidity current sediment waves on the submarine slopes of the western Canary Islands. *Mar. Geol.* 163, 185–198.
- Wynn, R.B., Weaver, P.P.E., Ercilla, G., Stow, D.A.V., Masson, D.G., 2000b. Sedimentary processes in the Selvage sediment-wave field, NE Atlantic: new insights into the formation of sediment waves by turbidity currents. *Sedimentology* 47, 1181–1197.
- Yoon, S.H., Chough, S.K., 1995. Regional strike slip in the eastern continental margin of Korea and its tectonic implications for the evolution of Ulleng Basin, East Sea (Sea of Japan). *Bull. Geol. Soc. Am.* 107, 83–97.
- Yoon, S.H., Lee, H.J., Han, S.J., Kim, S.R., 1996. Quaternary sedimentary processes on the east Korean continental slope. *J. Geol. Soc. Korea* 32, 250–266 (in Korean).